TRANSVERSE VELOCITY MEASUREMENT

Prepared for:

George C. Marshall Space Flight Center
Marshall Space Flight Center, Alabama 35812

TECHNOLOGY DEVELOPMENT CORPORATION

TDC-82-004

TRANSVERSE VELOCITY MEASUREMENT

Final Report

21 May 1982

Contract NAS8-34745

For the Period of 1 March through 21 May 1982

Prepared for:

George C. Marshall Space Flight Center
Marshall Space Flight Center, Alabama 35812

Prepared by:

Technology Development Corporation
4717 University Dr., Suite 114
Huntsville, Alabama 35805

TABLE OF CONTENTS

LIST OF ILLUSTRATIONS

TRANSVERSE VELOCITY MEASUREMENT

1. INTRODUCTION

Carbon dioxide (CO_2) laser Doppler lidar systems have been employed for several years in the remote measurement of wind velocities. These systems have been limited to obtaining the line-of-sight velocity component only. There have been various configurations devised for obtaining the cross velocity component but they were complex and difficult to align. Recent studies indicate that it may be possible to extract this cross velocity component utilizing an appropriate detector array configuration. This will allow determination of the three dimensional characteristics of the wind with conventional Doppler lidar systems.

2. EXPERIMENT DESCRIPTION

The experimental arrangement for measuring the transverse velocity component is shown in Figure 1. A CO_2 laser of conventional design with an output of three watts was used in the beginning but the power level proved to be insufficient and a CO_2 waveguide laser putting out seven watts was substituted. The homodyned signal from the detector using the waveguide laser was acceptable and appeared essentially no different in quality from that of the conventional laser indicating a beam profile basically Gaussian.

The receiver used in these measurements utilizes a twelve-element array of Mercury Cadmium Telluride (HgCdTe) photodiodes. The arrangement of these photodiodes is shown in Figure 2. The inner four elements were primarily used, with the elements in the outer ring being used to further verify measurements made with the inner four. Four wideband preamplifiers with associated bias electronics completed the receiver.

The Doppler signal from a given preamplifier was applied to a spectrum analyzer. The spectrum analyzer was centered on the signal with zero scan width and the video output was fed into a signal correlator. Only two spectrum analyzers were available so only two receiver channels were utilized at one time.

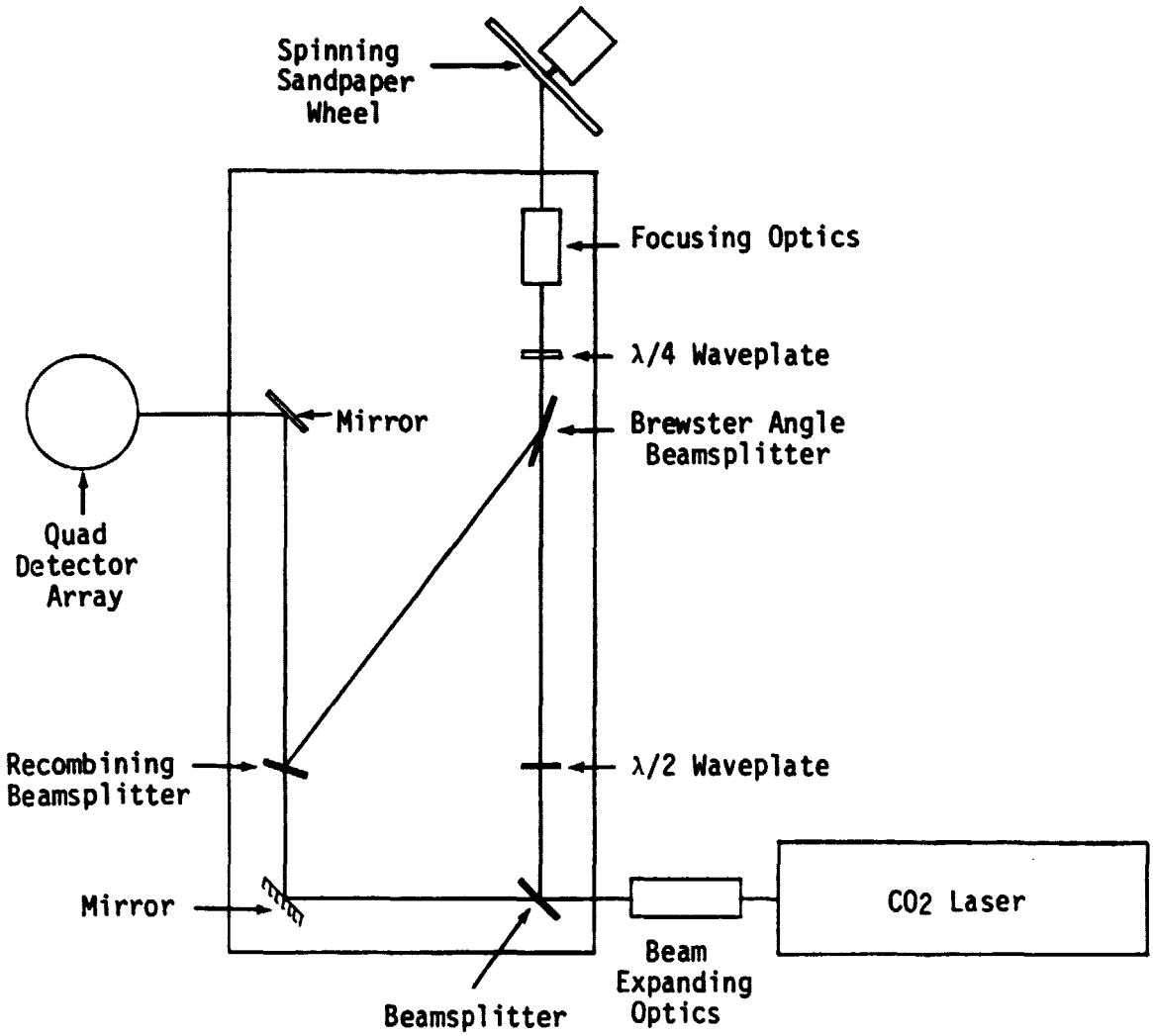

Figure 1. Experimental Arrangement for Measuring Transverse Velocity Component

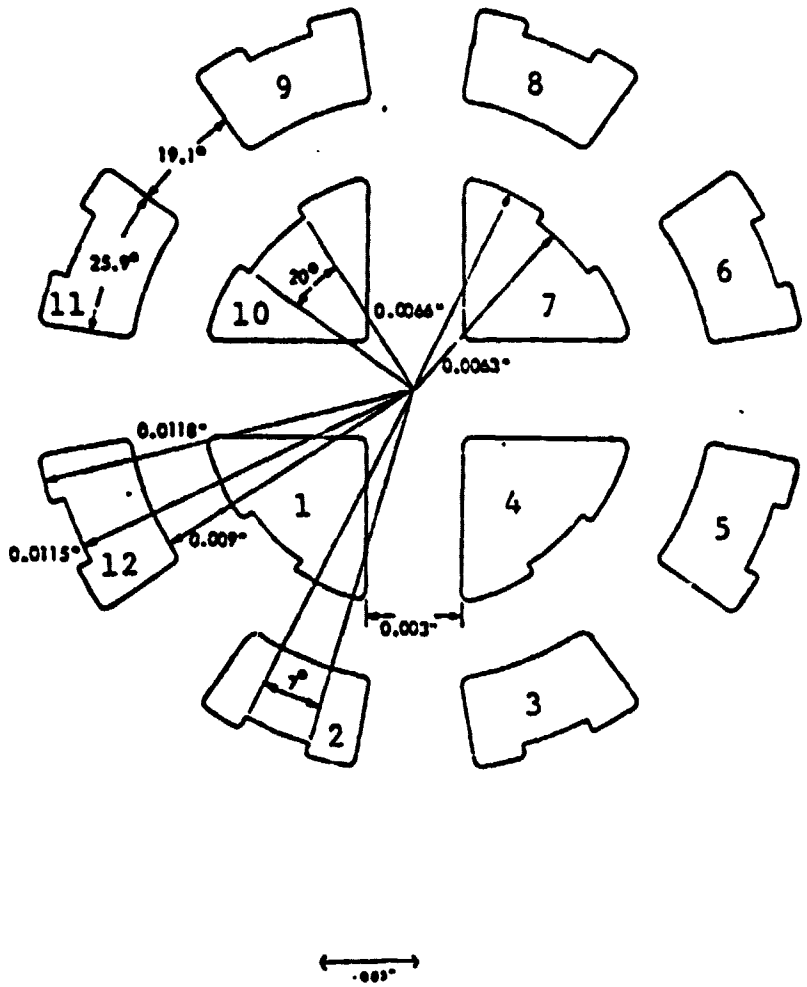

Figure 2. Twelve-Element Array of HgCdTe Photodiodes

3. EXPERIMENT RESULTS

The Doppler return from the spinning sandpaper wheel was measured for various angles of incidence. This data is shown in Table 1. The video output from the two spectrum analyzers was fed into the signal correlator as described in Section 2. Figure 3 shows examples of auto-correlated signals. The transverse velocity component can be extracted when the signal from two different detector elements are compared or cross-correlated. Examples of cross-correlation signals are shown in Figure 4.

When the cross-correlation signals were used to compute the transverse velocity component, inconsistent results indicated a problem. It was discovered that the detector array being used to make the measurements did not conform to the layout in Figure 2. A second array which did conform to the description was used and a complete set of data was obtained. Figure 5 shows the spectrum analyzer signals from detector element #3 and #8. Figure 6 shows the auto-correlation and cross-correlation signals for various sandpaper wheel and Doppler frequencies. Theta (θ) is the angle the laser beam makes with the normal to the wheel surface, and f_D is the result in Doppler frequency as read on the spectrum analyzer.

Table 1. Doppler Return vs. Angle of Incidence

Angle of Incidence θ (deg)	Center Frequency f_o (KHz)	Bandwidth 3dB Δf (KHz)	Bandwidth Full Δf_F (KHz)	Signal-to-Noise Ratio SNR (dB)
5	280	38	90	33
10	560	52	160	36
15	840	70	200	36
20	1080	75	240	34
25	1330	90	280	31
30	1600	120	315	29
35	1800	130	400	28
40	2000	150	430	25
45	2200	160	450	25

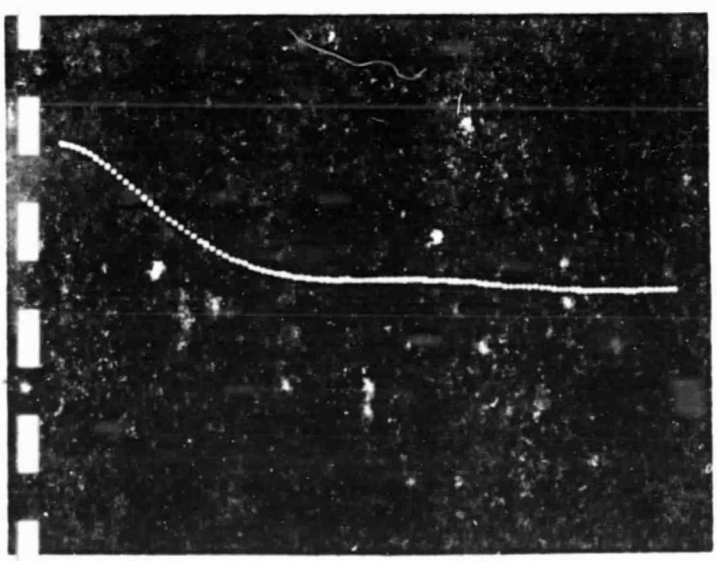

$\theta = 5^o$

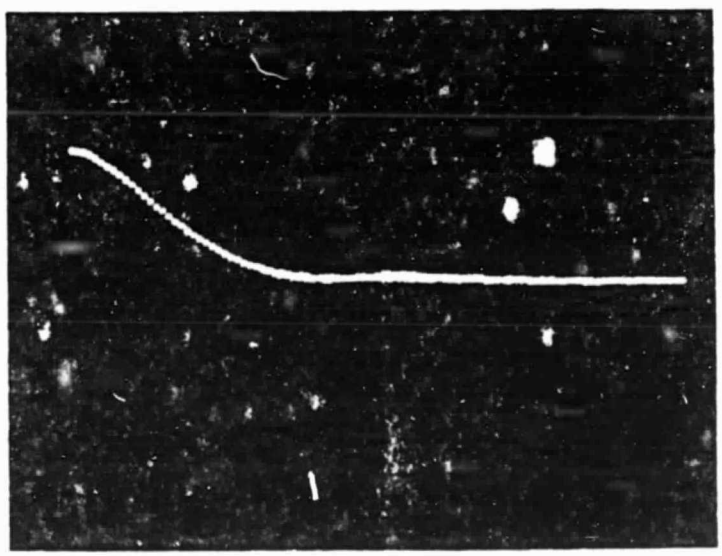

$\theta = 10^o$

Figure 3. Autocorrelation of Doppler Signal

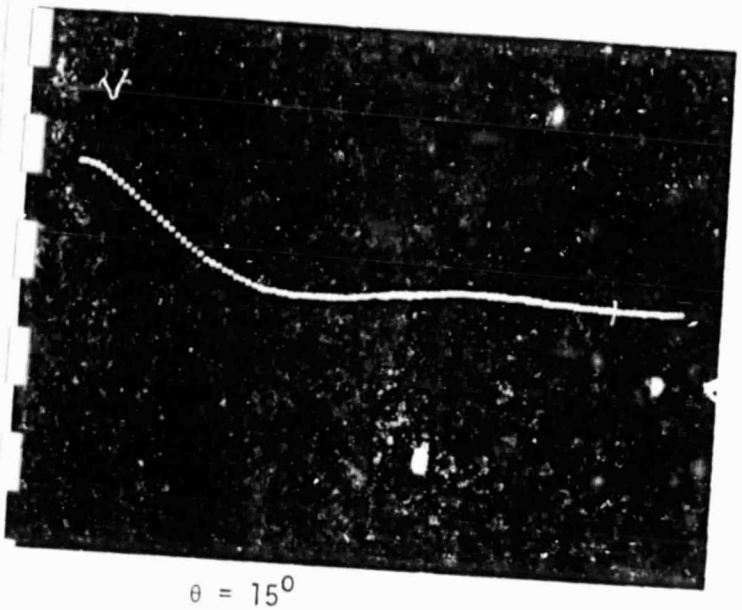

$\theta = 15^{o}$

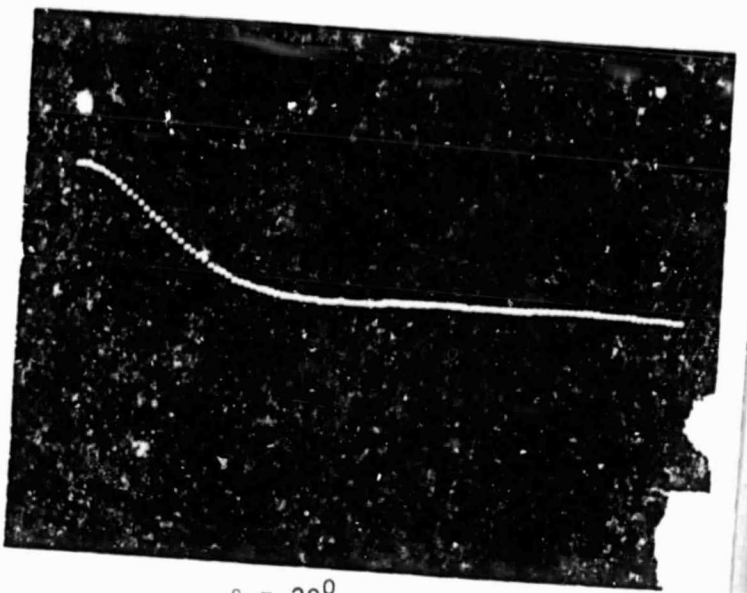

$\theta = 20^{o}$

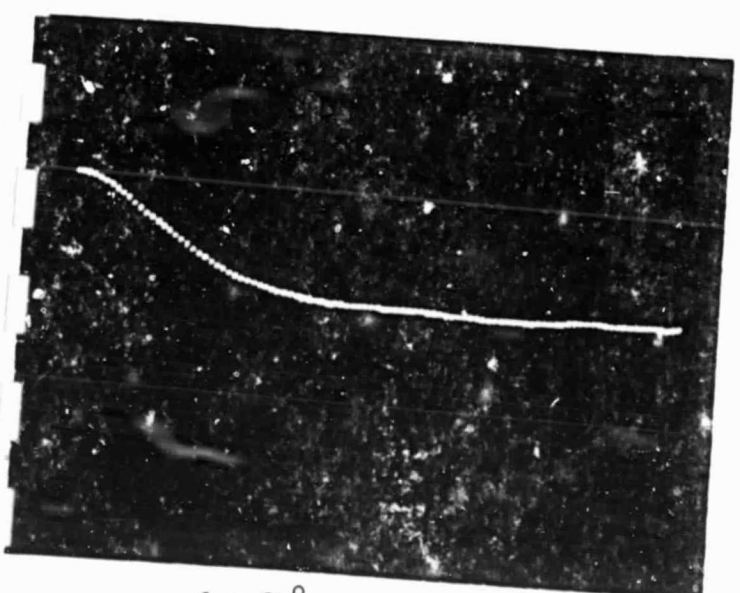

$\theta = 25^{o}$

$\theta = 30^{o}$

Figure 3. (Continued)

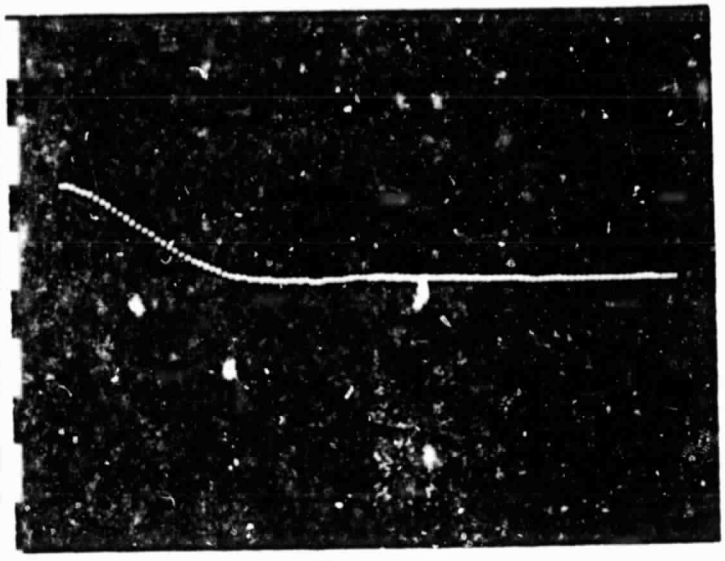

$\theta = 35^{o}$

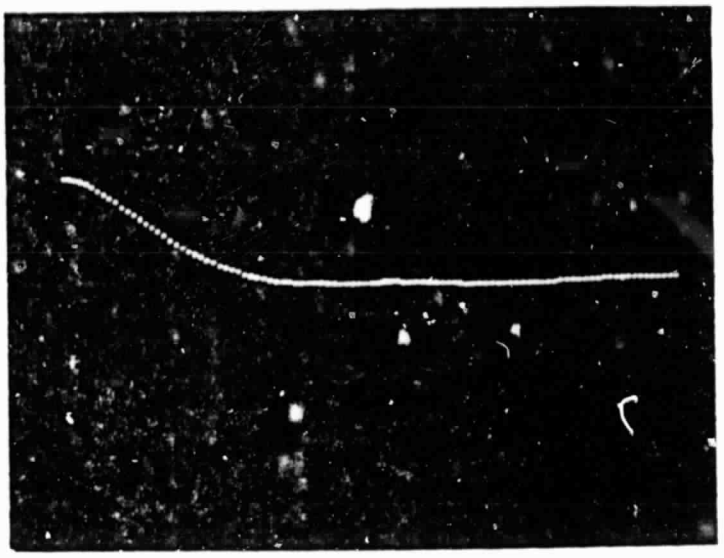

$\theta = 40^{o}$

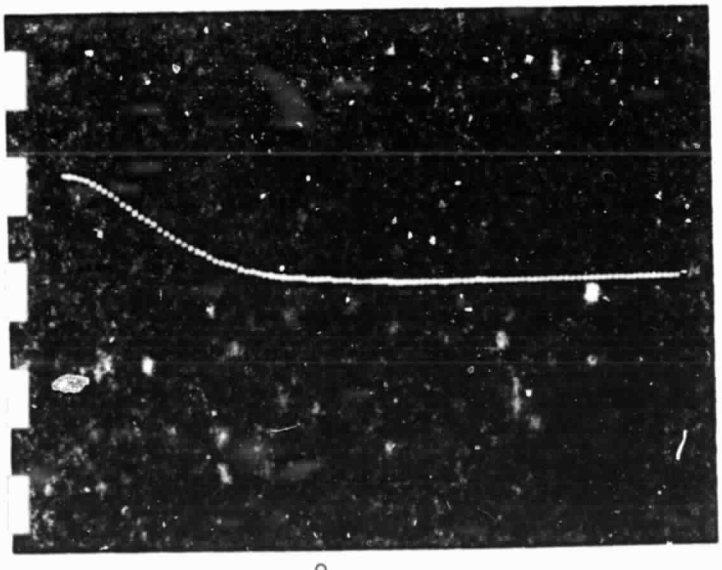

$\theta = 45^{o}$

Figure 3. (Continued)

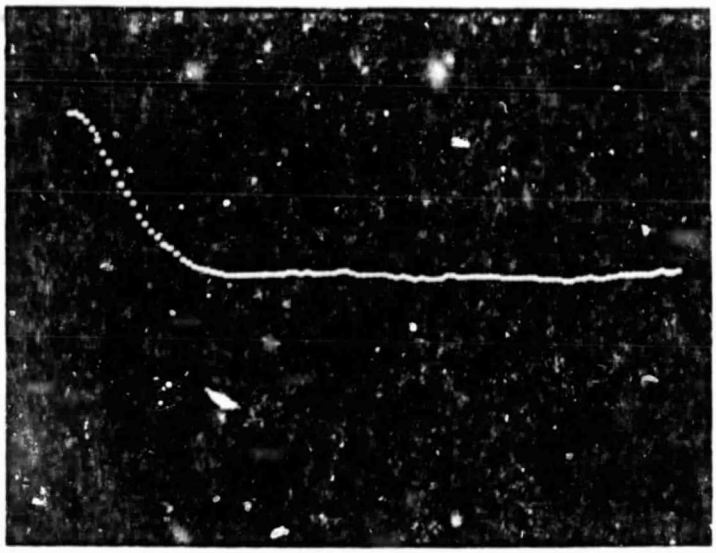

Element #8 Self Correlation

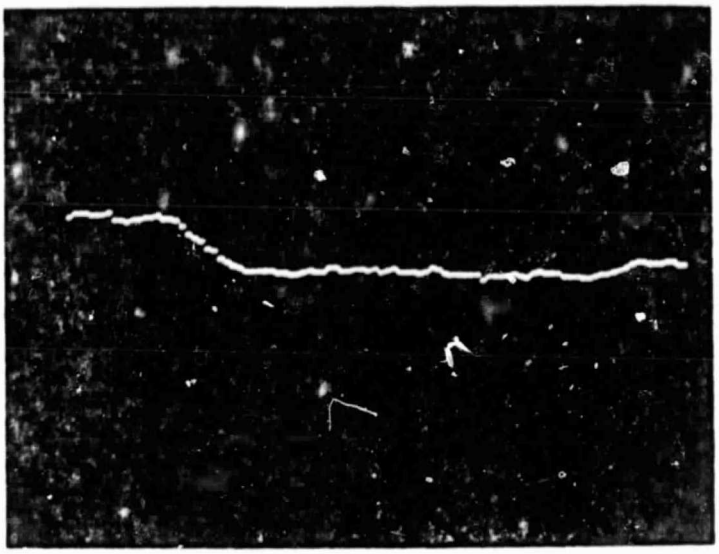

Cross Correlation of #8 with #1
#8 Delayed

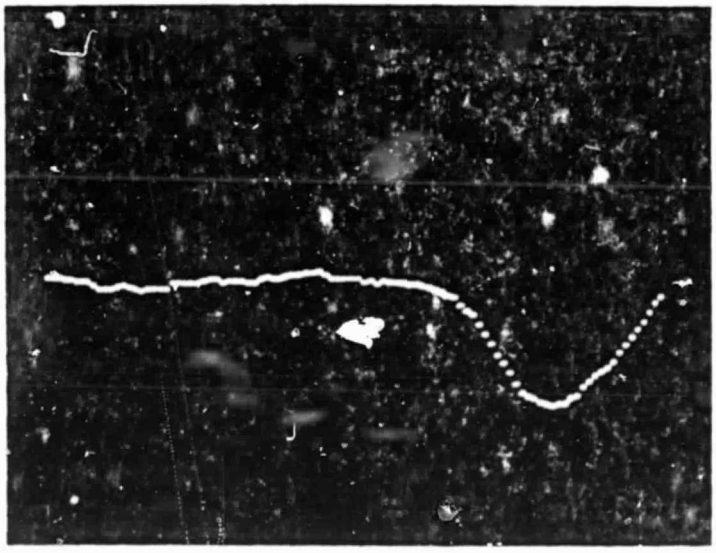

Cross Correlation of #8 with #2
#8 Delayed

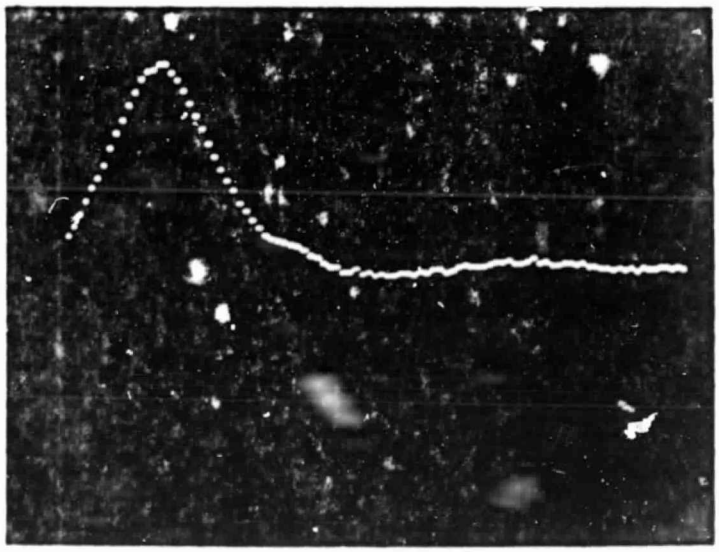

Cross Correlation of #8 with #3
#8 Delayed

Figure 4. Correlator Signals from Twelve-Element Array of Photodiodes

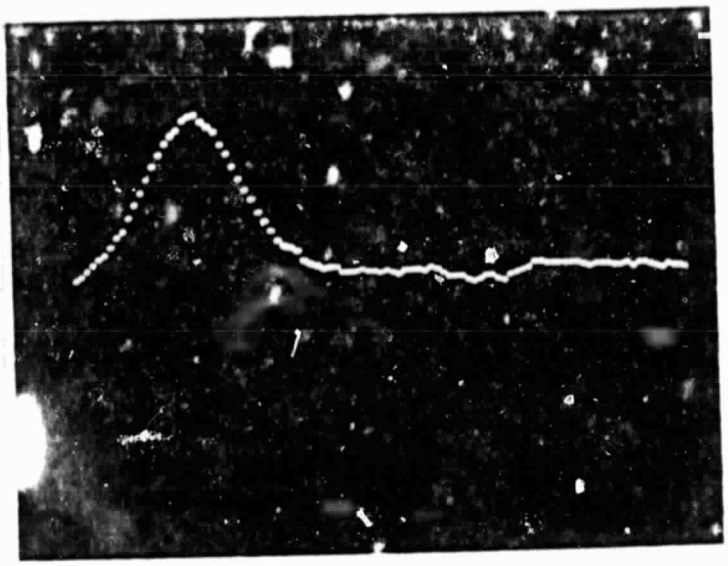

Cross Correlation of #8 with #4
#8 Delayed

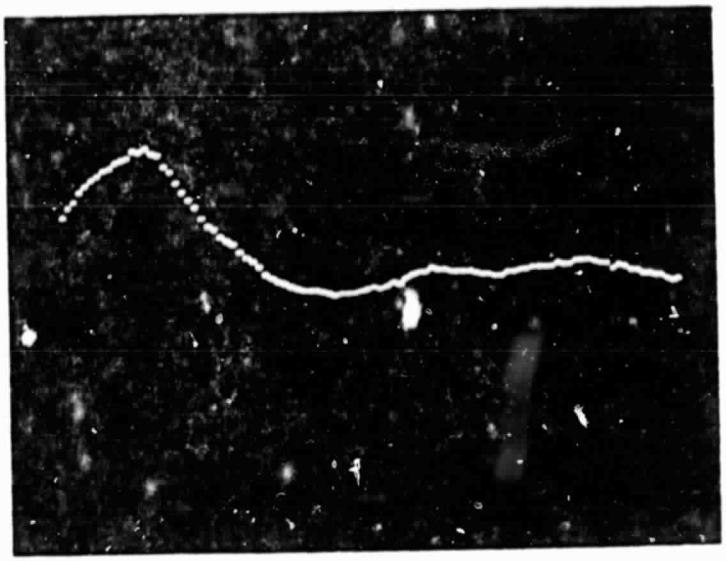

Cross Correlation of #8 with #5
#8 Delayed

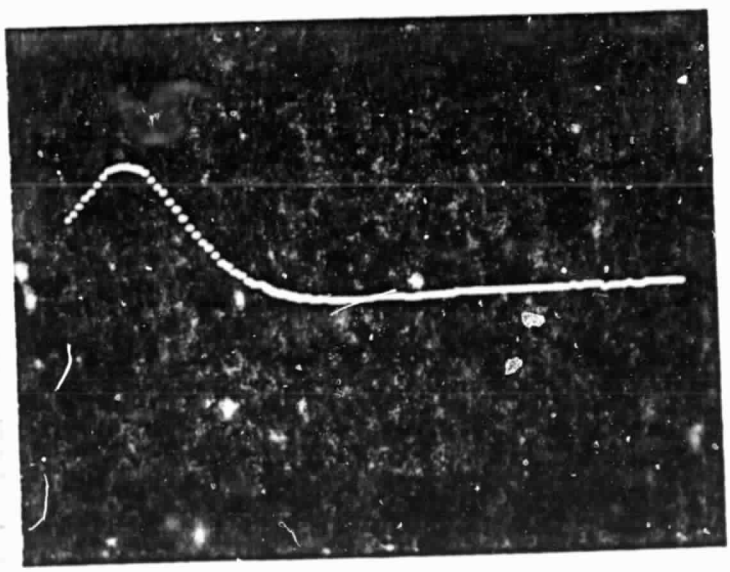

Cross Correlation of #8 with #6
#8 Delayed

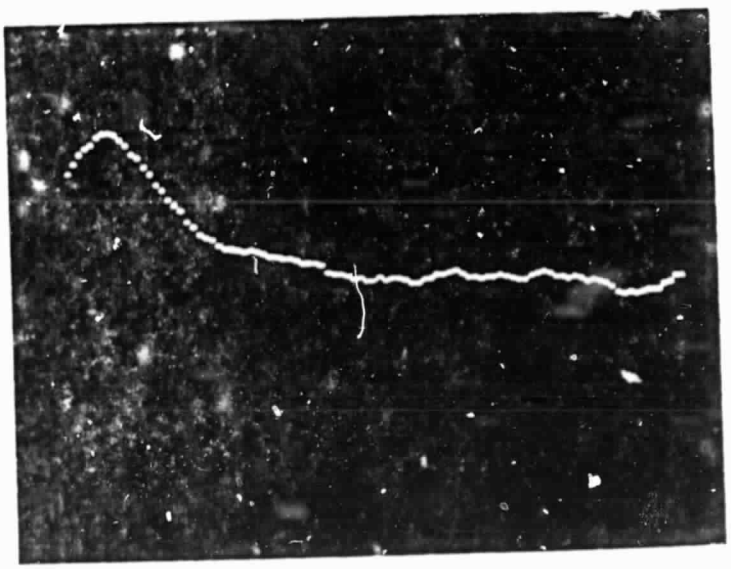

Cross Correlation of #8 with #7
#8 Delayed

Figure 4. (Continued)

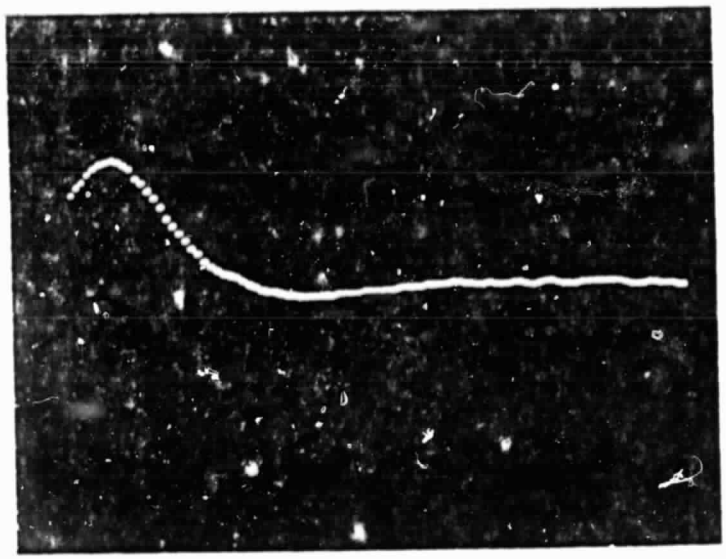

Cross Correlation of #8 with #9
#8 Delayed

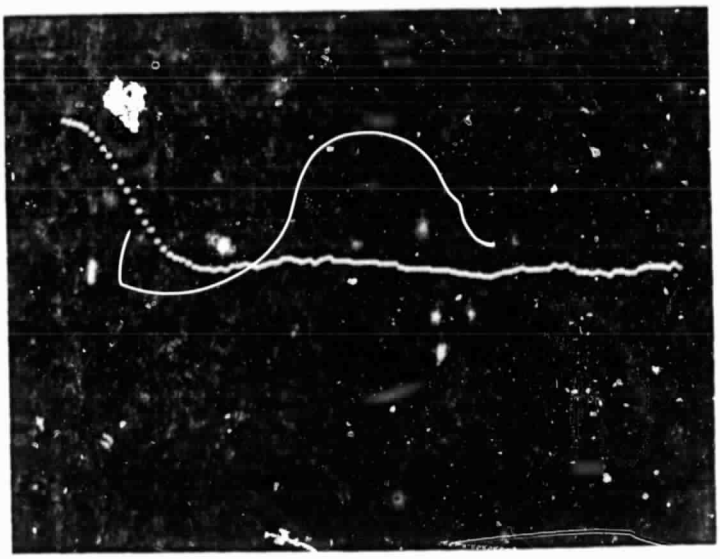

Cross Correlation of #8 with #10
#8 Delayed

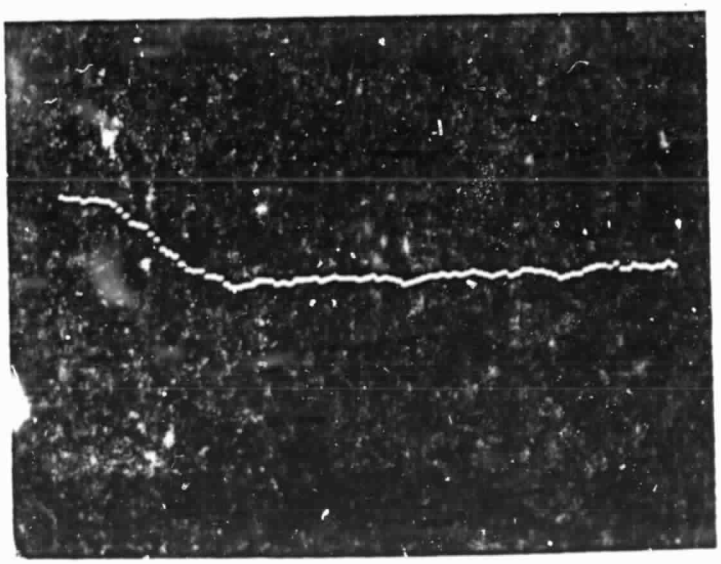

Cross Correlation of #8 with #11
#8 Delayed

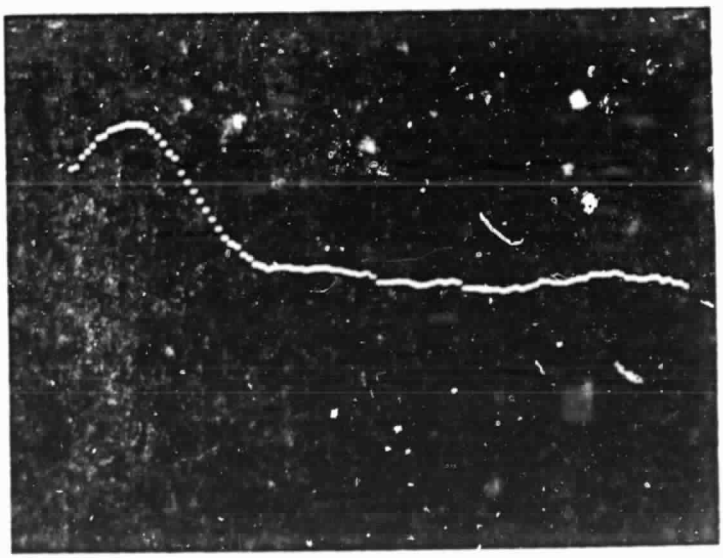

Cross Correlation of #8 with #12
#8 Delayed

Figure 4. (Continued)

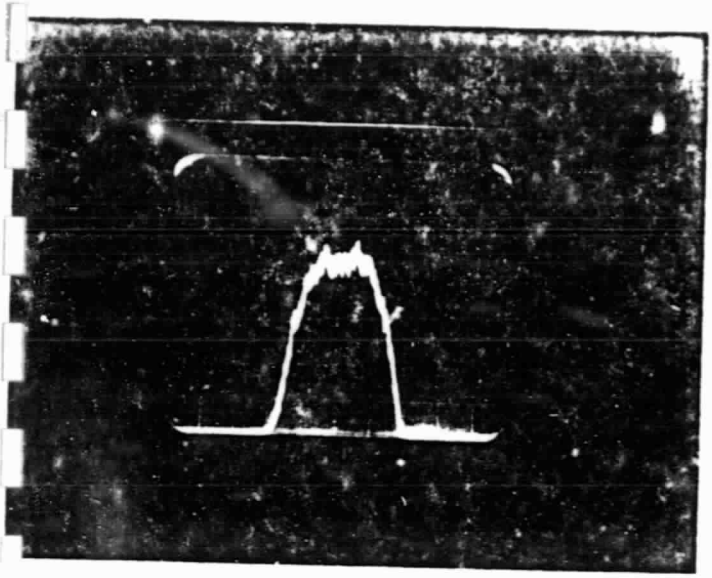

#3, f_D=220KHz, θ=15°, 2dB/cm, 10KHz/cm

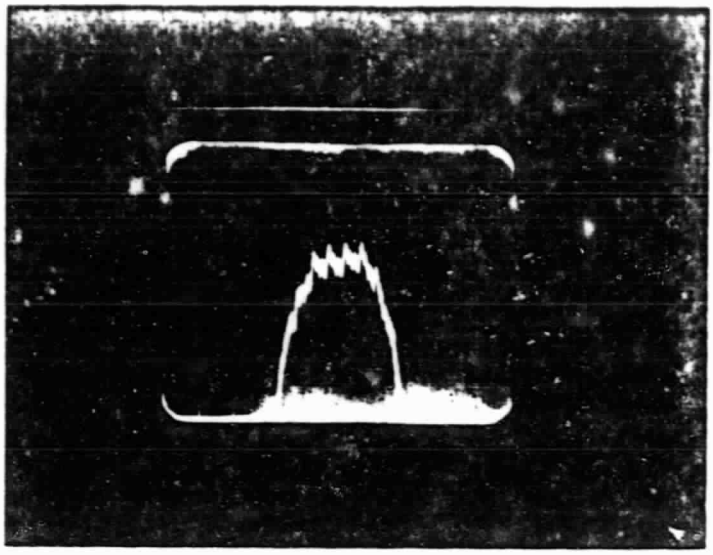

#3, f_D=370KHz, θ=15°, 2dB/cm, 10KHz/cm

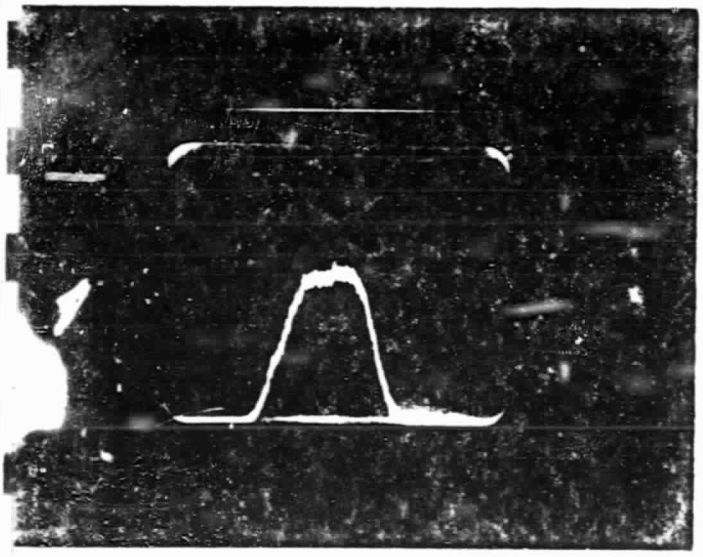

#3, f_D=300KHz, θ=20°, 2dB/cm, 10KHz/cm

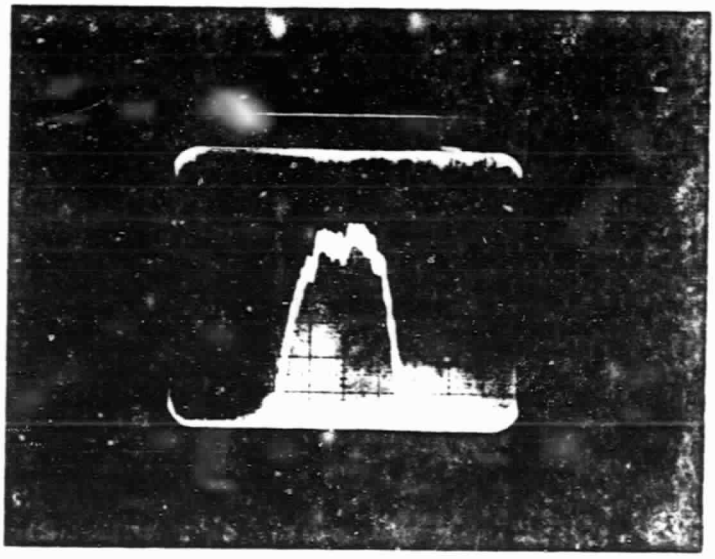

#3, f_D=440KHz, θ=30°, 2dB/cm, 10KHz/cm

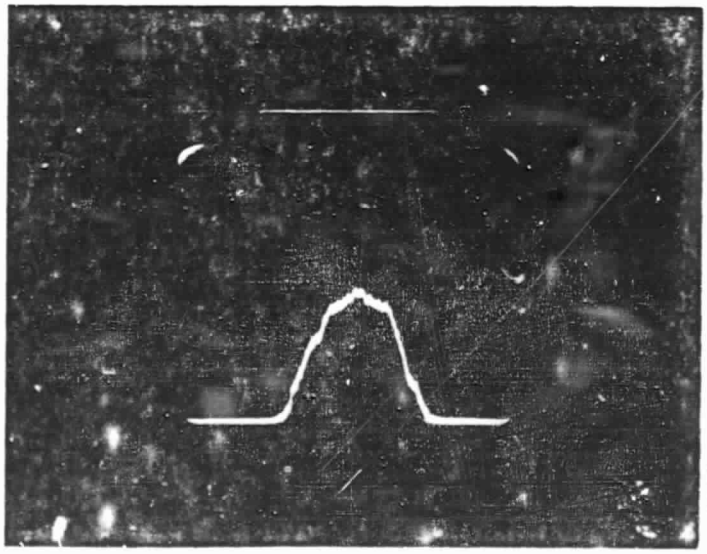

#3, f_D=960KHz, θ=60°, 2dB/cm, 10KHz/cm

Figure 5. Spectrum Analyzer Display of Doppler Signals

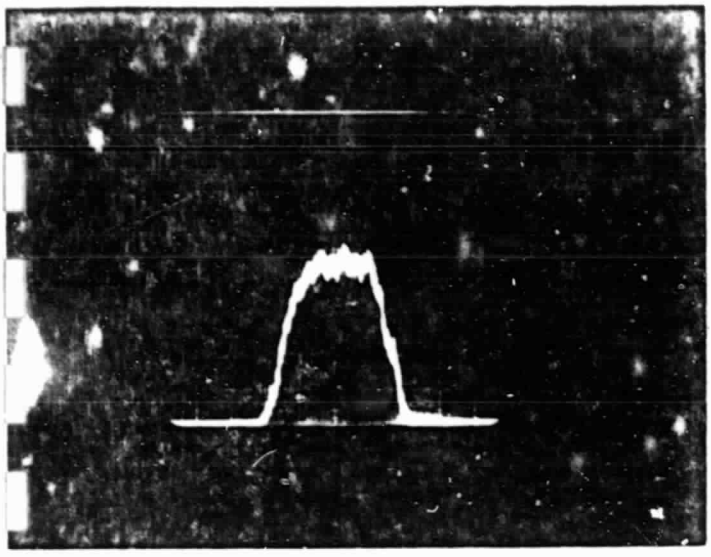

#8, f_D=400KHz, 2dB/cm, 10KHz/cm

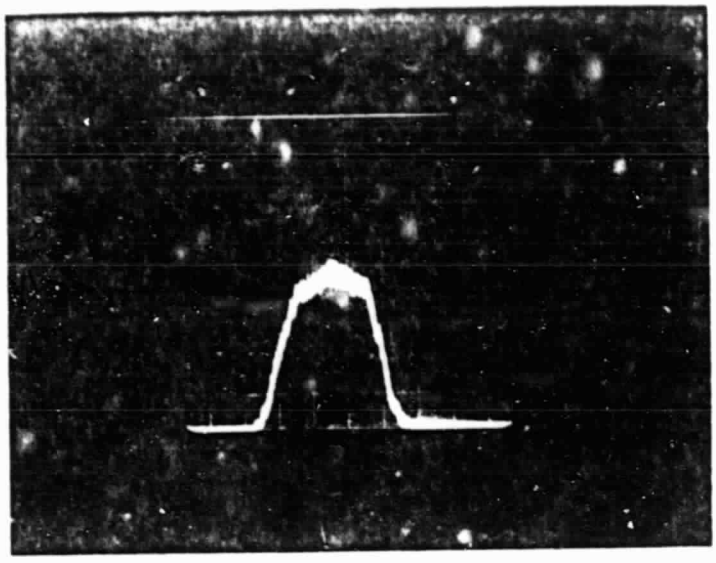

#8, f_D=600KHz, 2dB/cm, 10KHz/cm

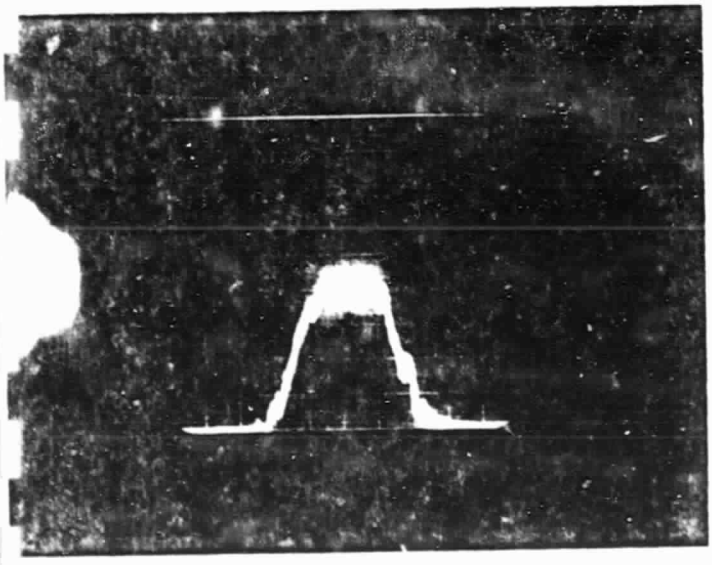

#8, f_D=800KHz, 2dB/cm, 10KHz/cm

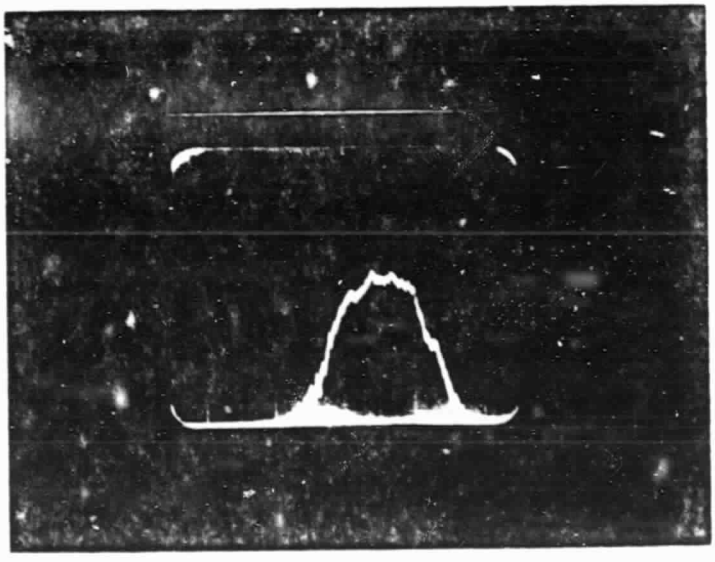

#8, f_D=1MHz, 2dB/cm, 10KHz/cm

Figure 5. (Continued)

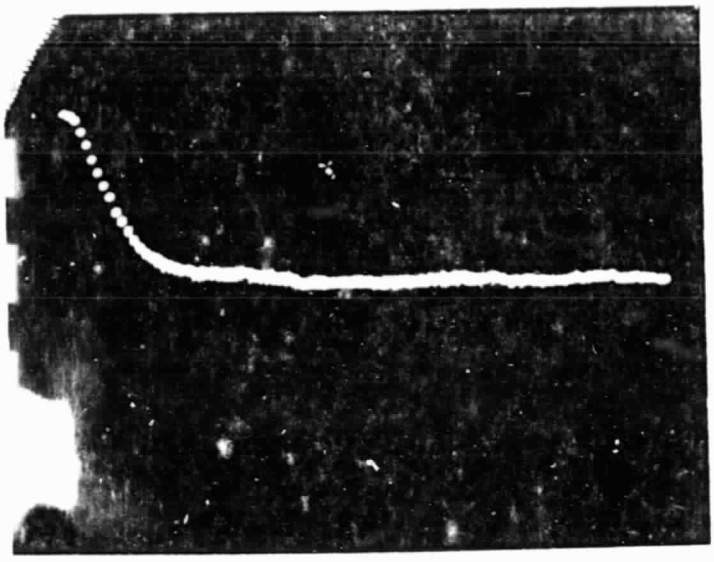

#3, f_D=800KHz, θ=45°

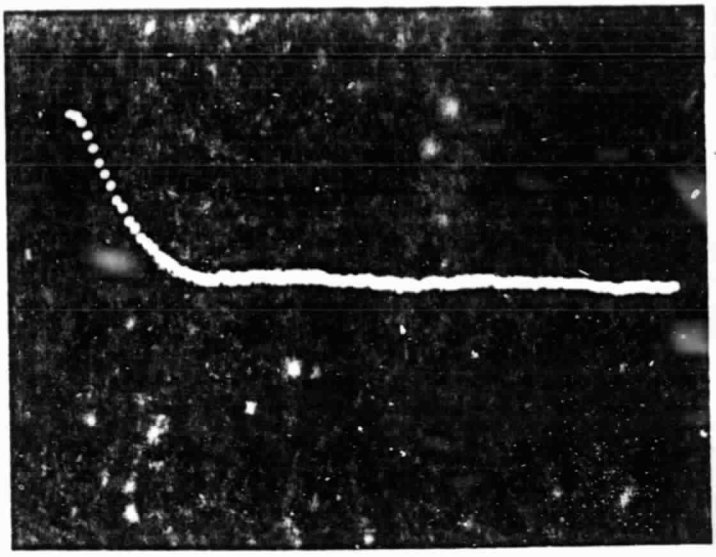

#8, f_D=800KHz, θ=45°

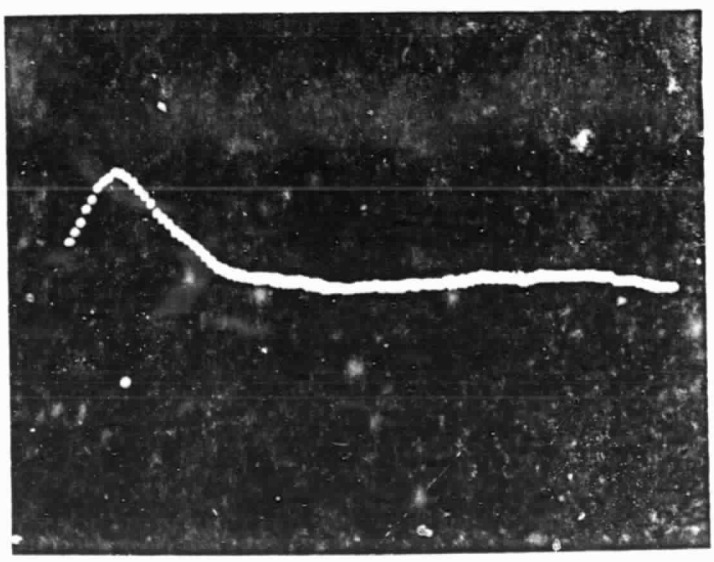

8x3 Delayed, f_D=800KHz, θ=45°

Figure 6. Correlator Signals for Various Wheel Angles

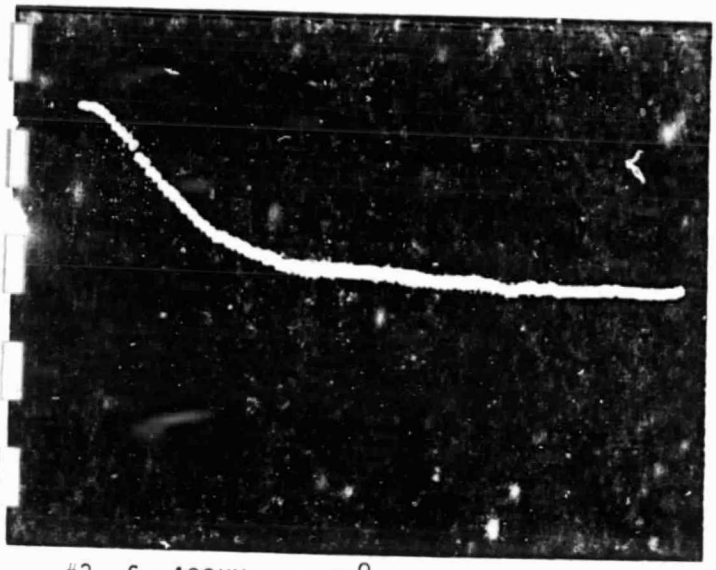

#3, f_D=400KHz, θ=45°

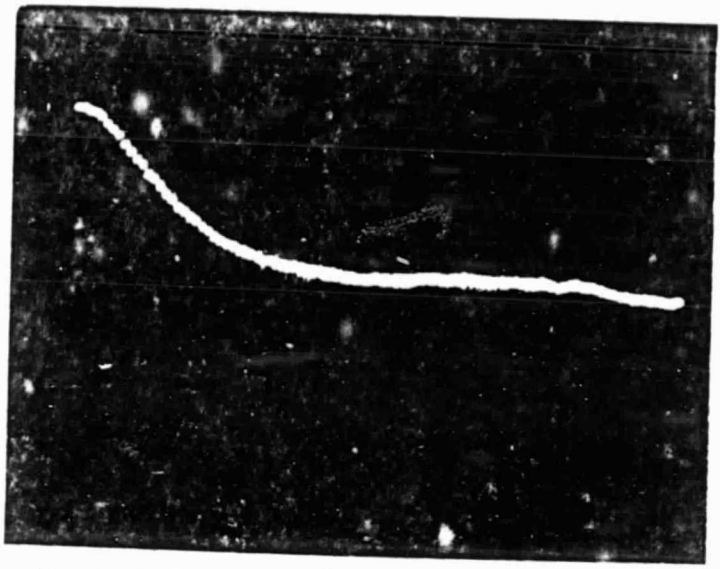

#8, f_D=400KHz, θ=45°

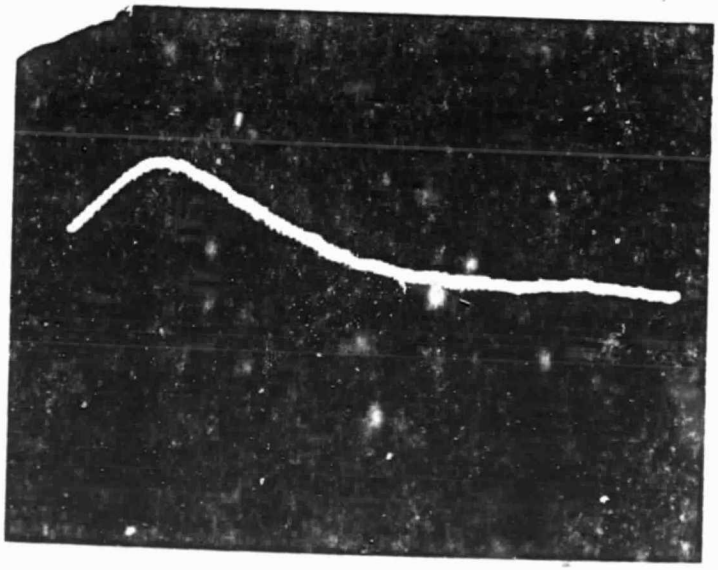

8x3 Delayed, f_D=400KHz, θ=45°

Figure 6. (Continued)

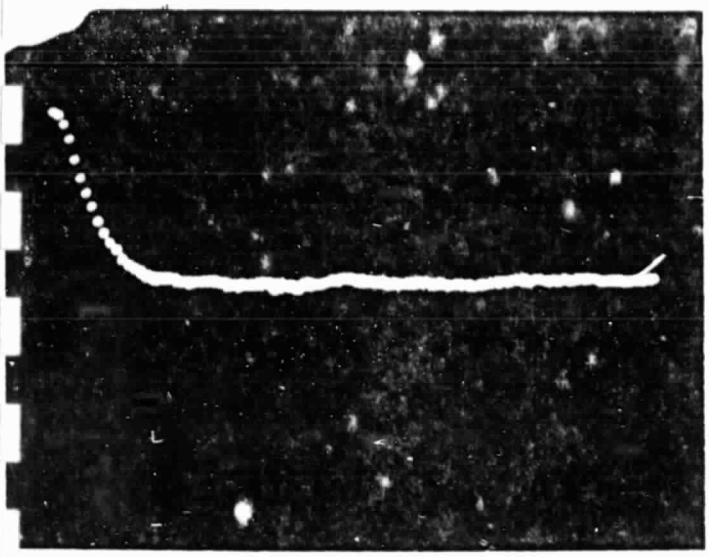

#3, f_D=1MHz, θ=45°

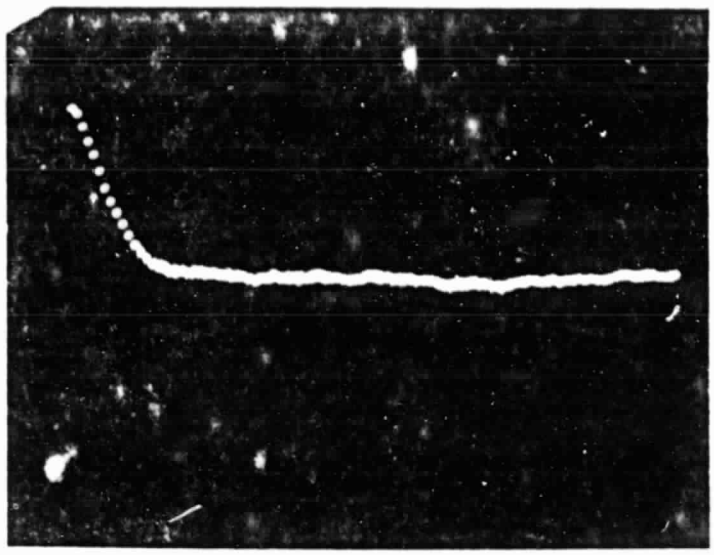

#8, f_D=1MHz, θ=45°

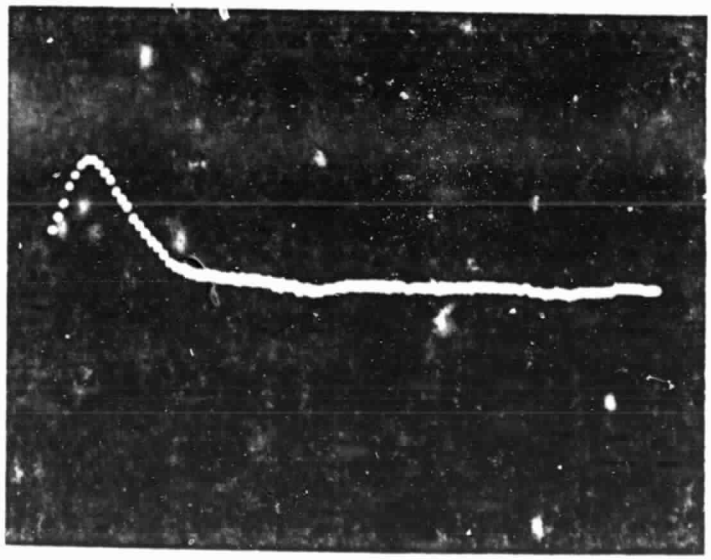

8x3 Delayed, f_D=1MHz, θ=45°

Figure 6. (Continued)

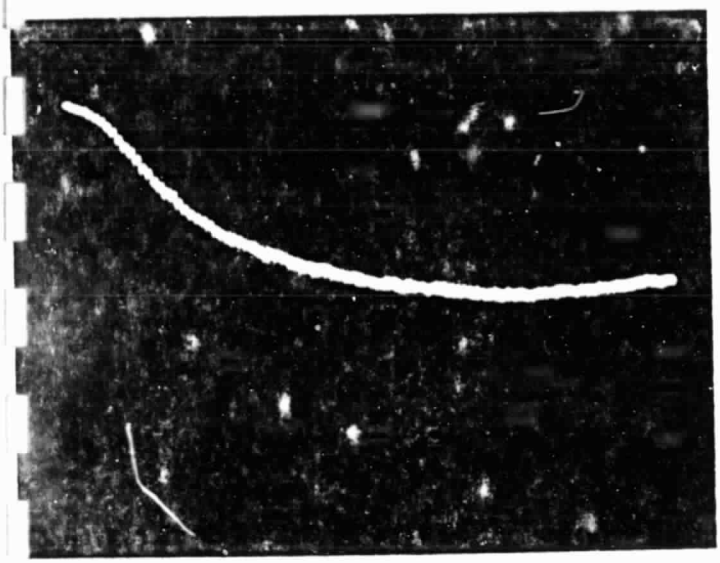

#3, f_D=300KHz, θ=20°

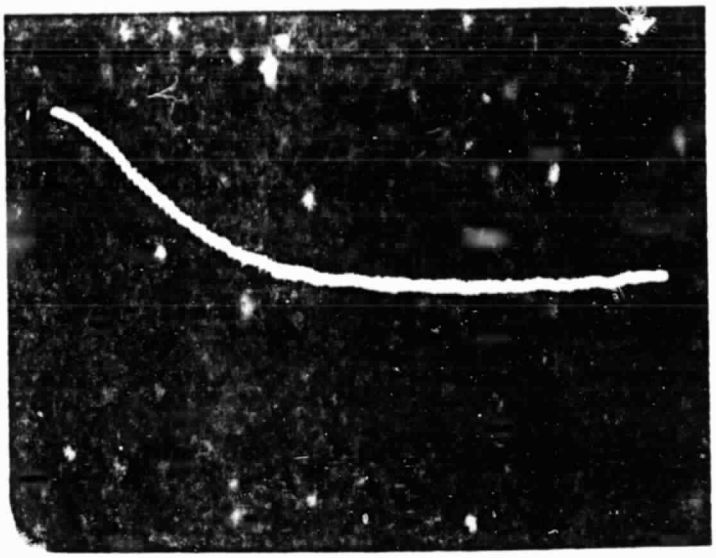

#8, f_D=300KHz, θ=20°

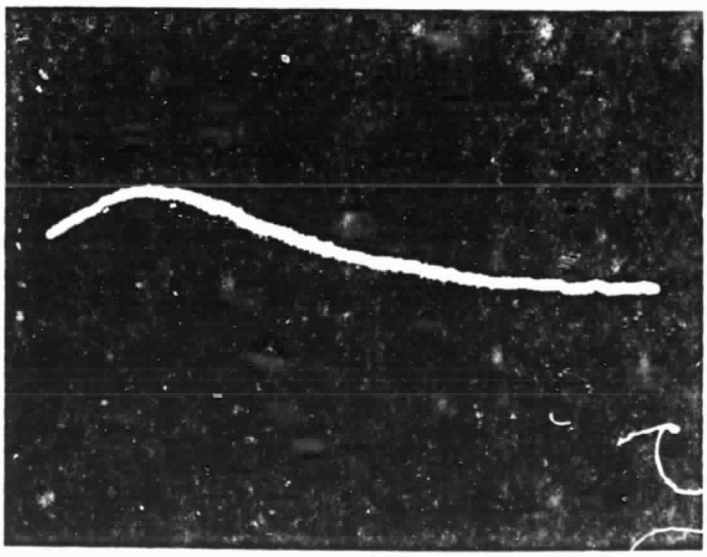

8x3 Delayed, f_D=300KHz, θ=20°

Figure 6. (Continued)

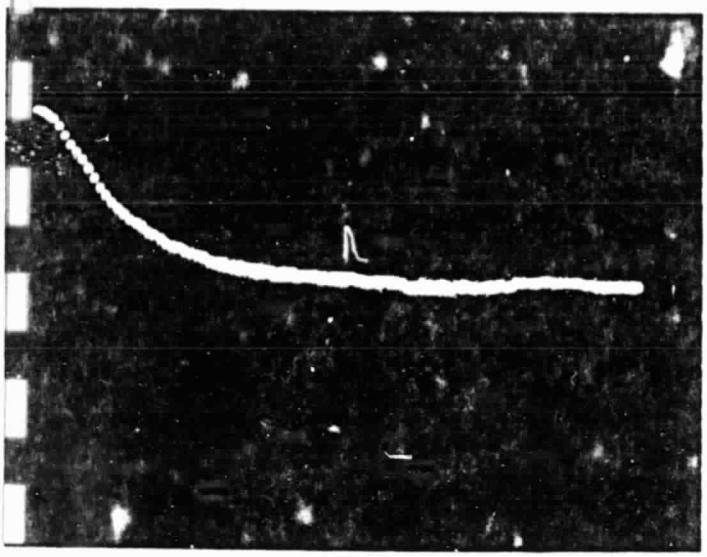

#3, f_D=440KHz, θ=30°

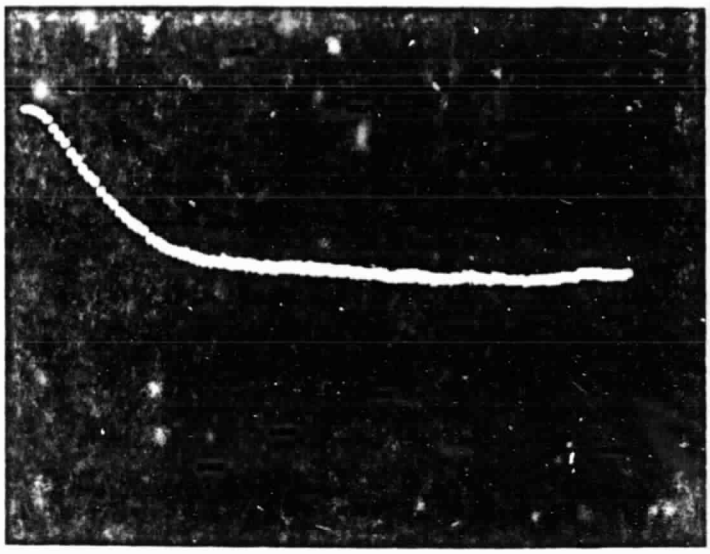

#8, f_D=440KHz, θ=30°

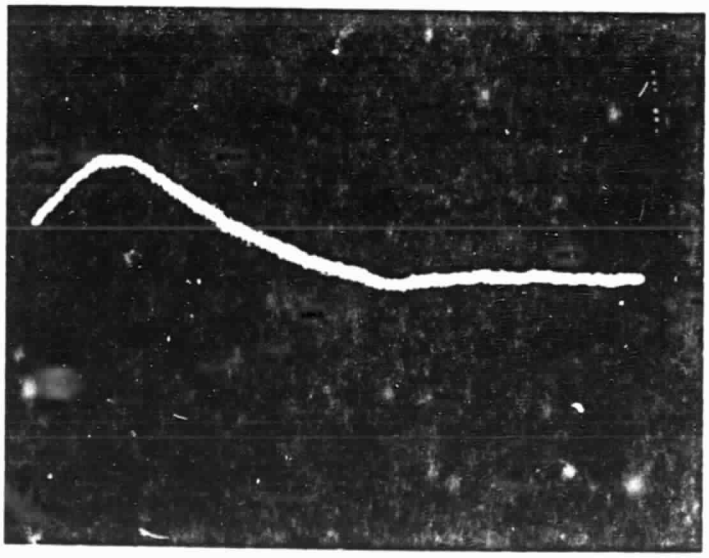

8x3 Delayed, f_D=440KHz, θ=30°

Figure 6. (Continued)

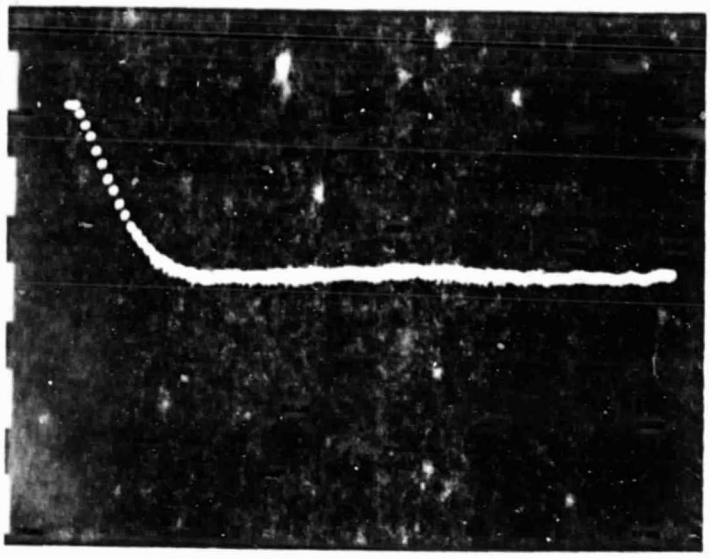

#3, f_D=960KHz, θ=60°

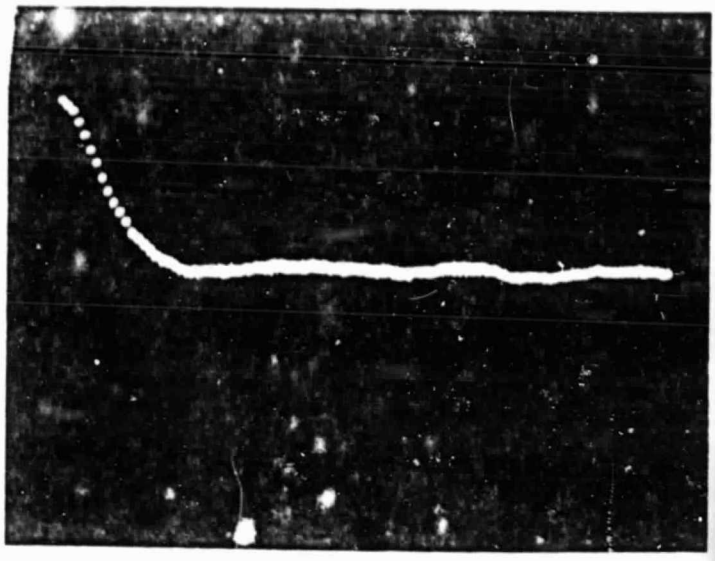

#8, f_D=960KHz, θ=60°

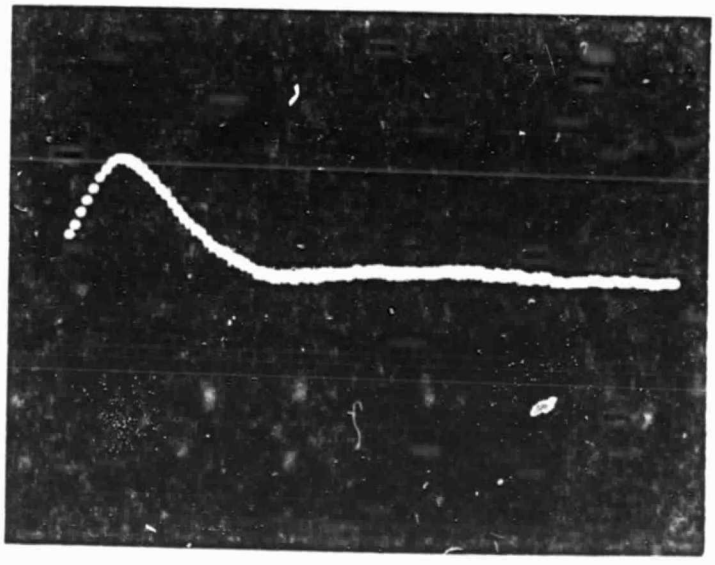

8x3 Delayed, f_D=960KHz, θ=60°

Figure 6. (Continued)

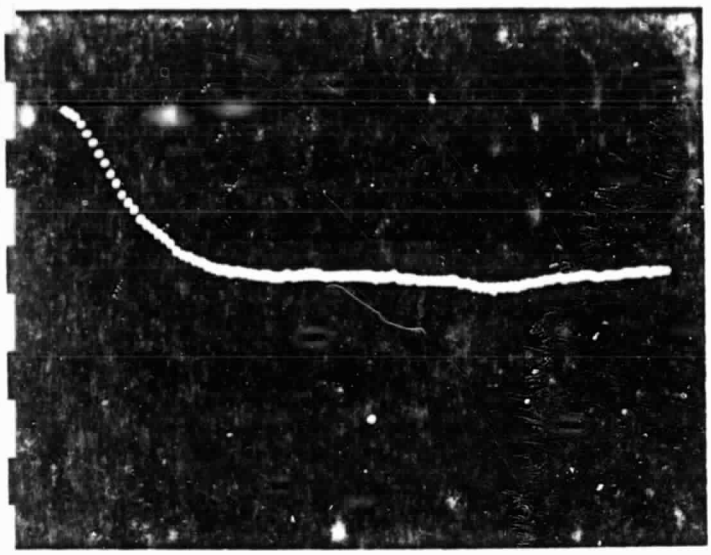

#3, f_D=600KHz, θ=45°

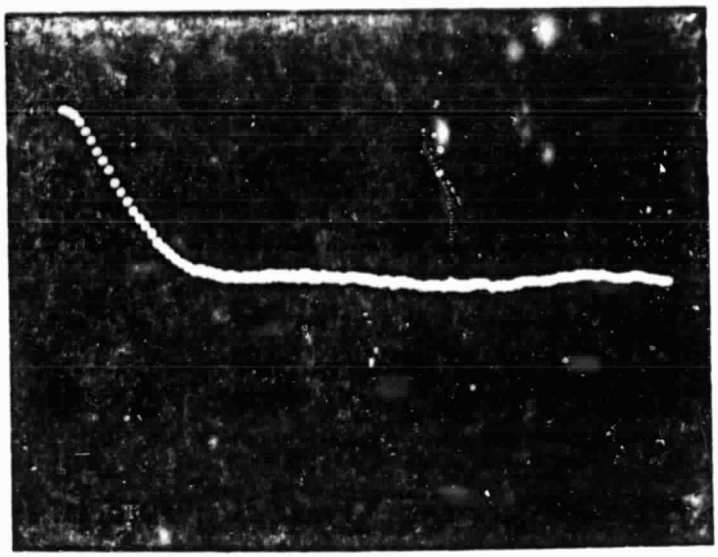

#8, f_D=600KHz, θ=45°

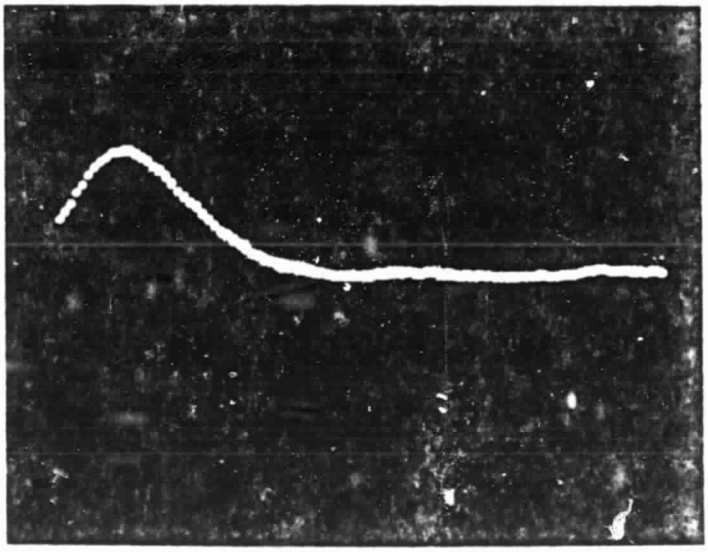

8x3 Delayed, f_D=600KHz, θ=45°

Figure 6. (Continued)

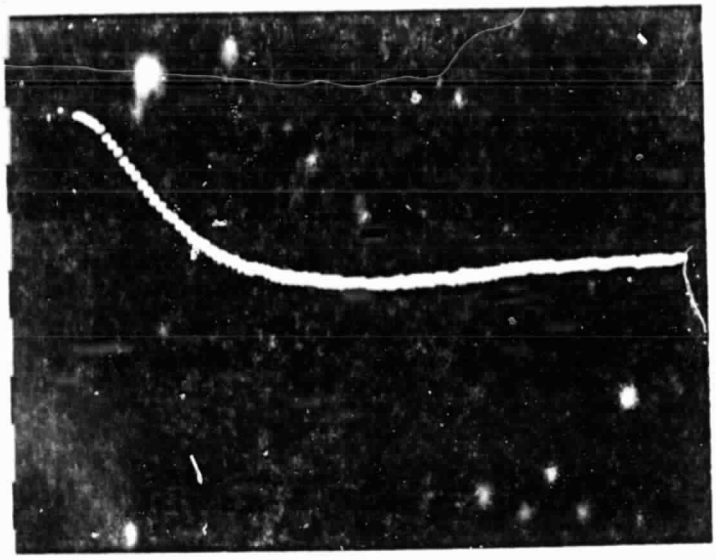

#3, f_D=370KHz, θ=25°

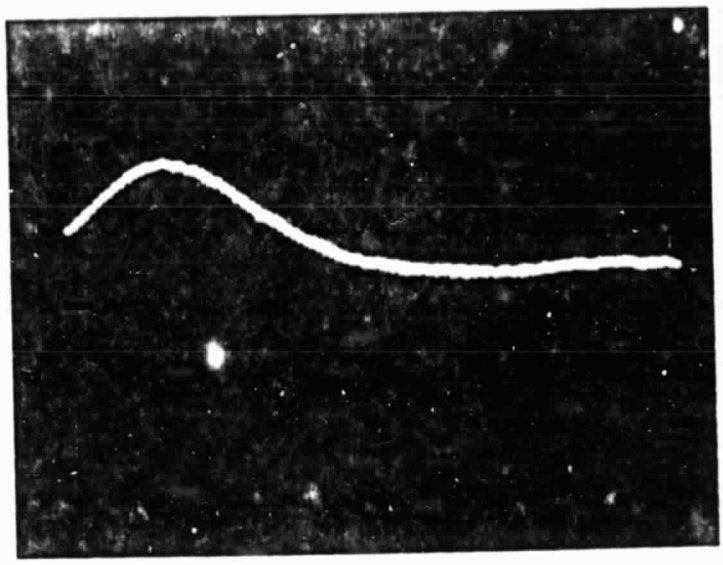

#8, f_D=370KHz, θ=25°

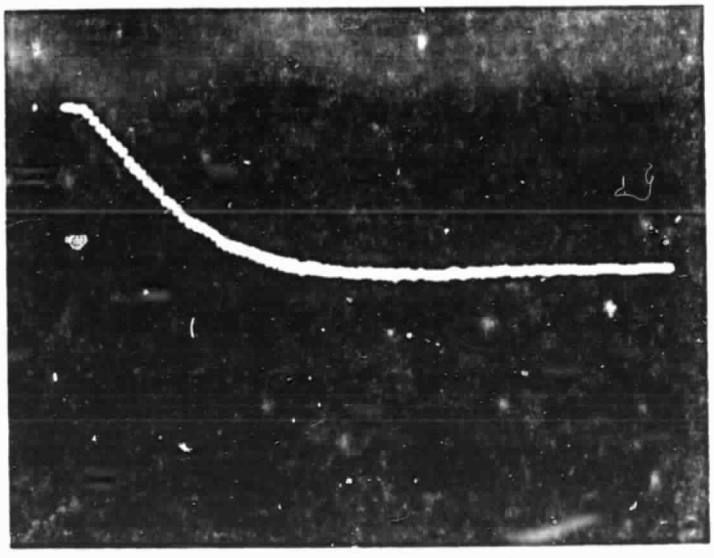

8x3 Delayed, f_D=370KHz, θ=25°

Figure 6. (Continued)

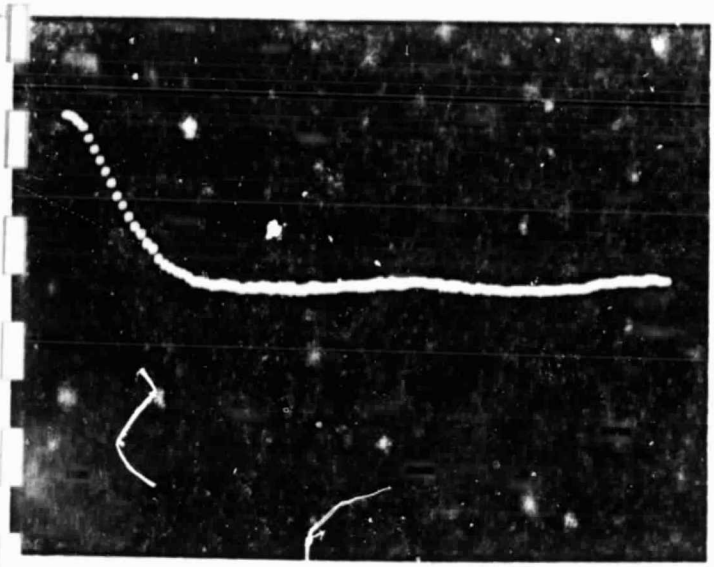

#4, f_D=600KHz, θ=45°

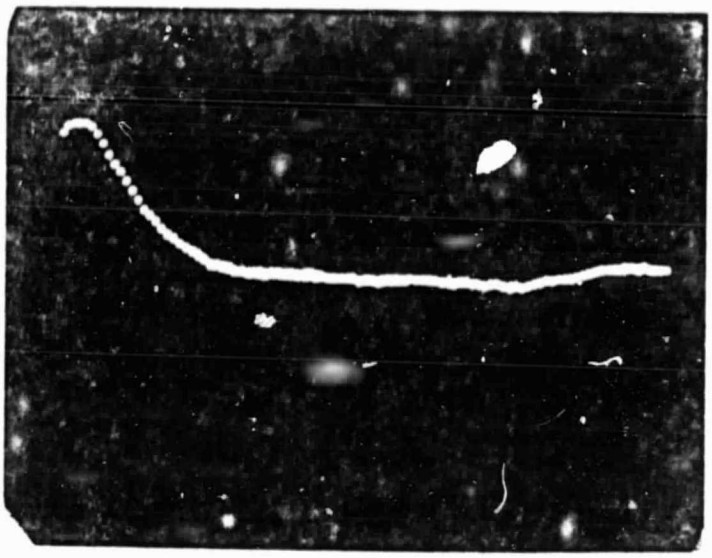

4x3 Delayed, f_D=600KHz, θ=45°

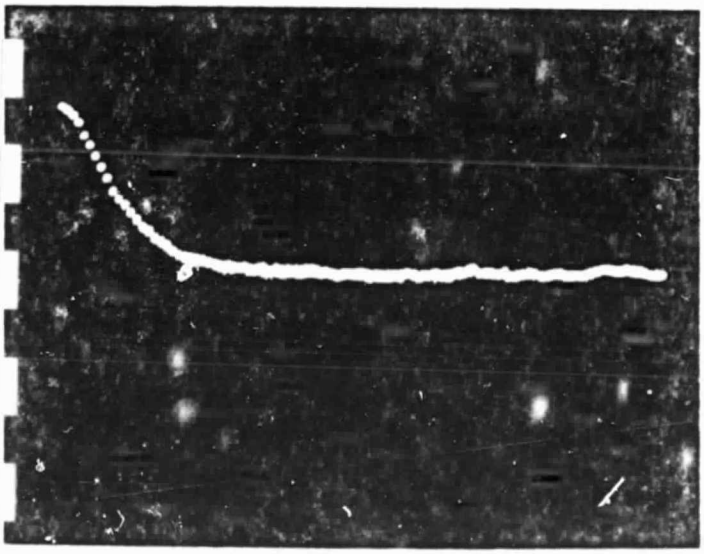

#7, f_D=600KHz, θ=45°

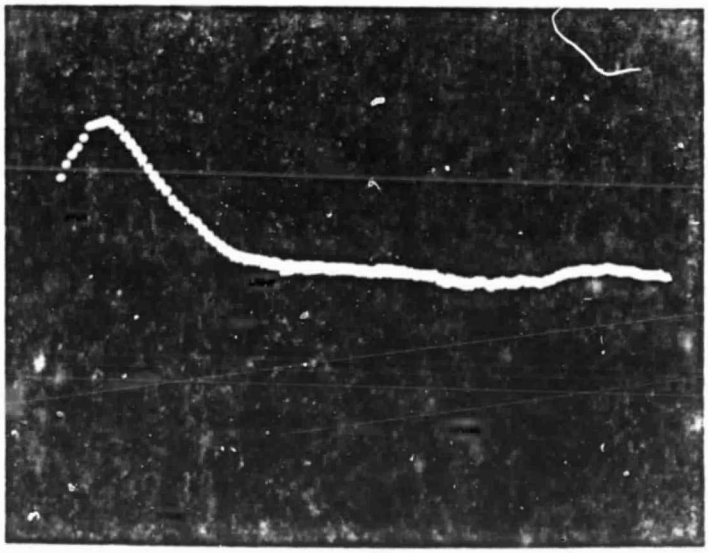

7x3 Delayed, f_D=600KHz, θ=45°

Figure 6. (Continued)

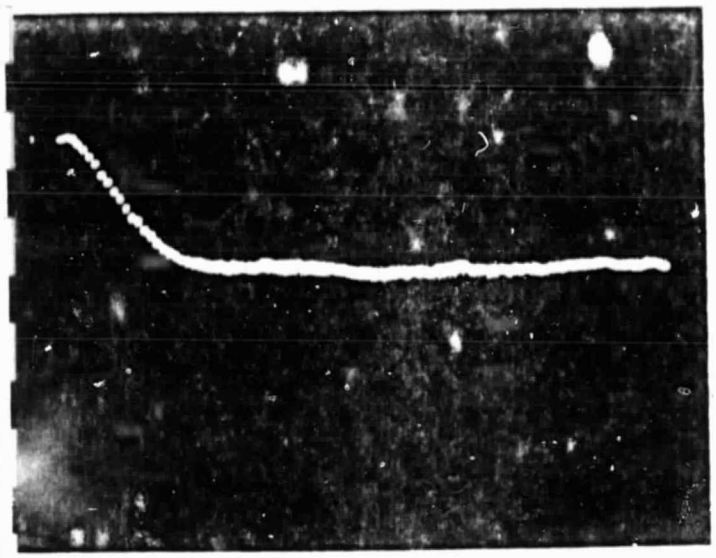

1x4 Delayed, f_D=600KHz, θ=45^o

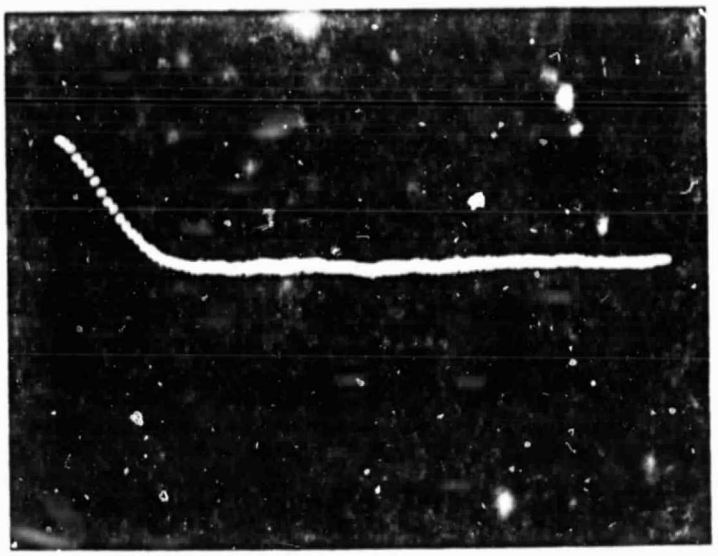

4x1 Delayed, f_D=600KHz, θ=45^o

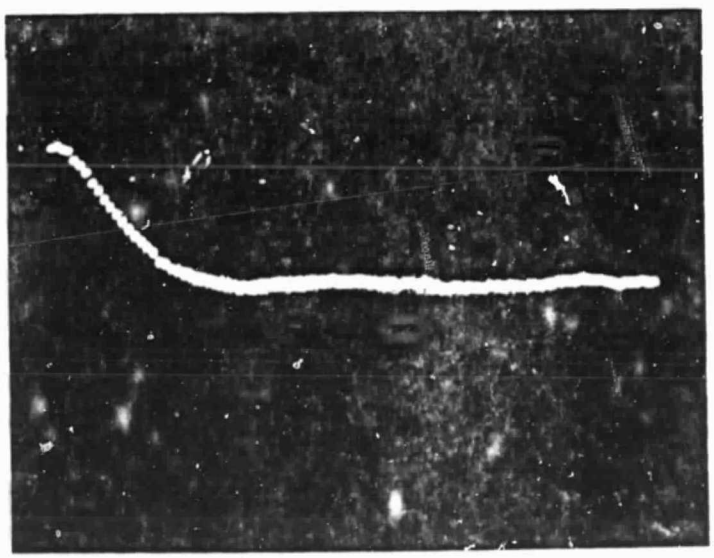

10x7 Delayed, f_D=600KHz, θ=45^o

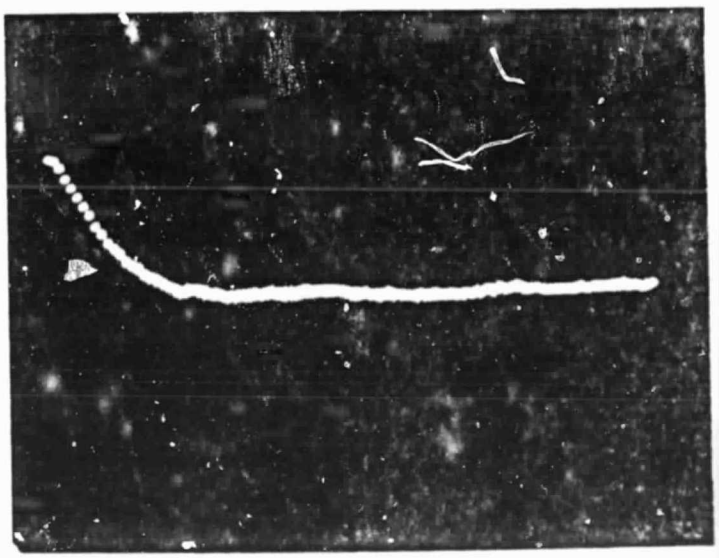

7x10 Delayed, f_D=600KHz, θ=45^o

Figure 6. (Continued)

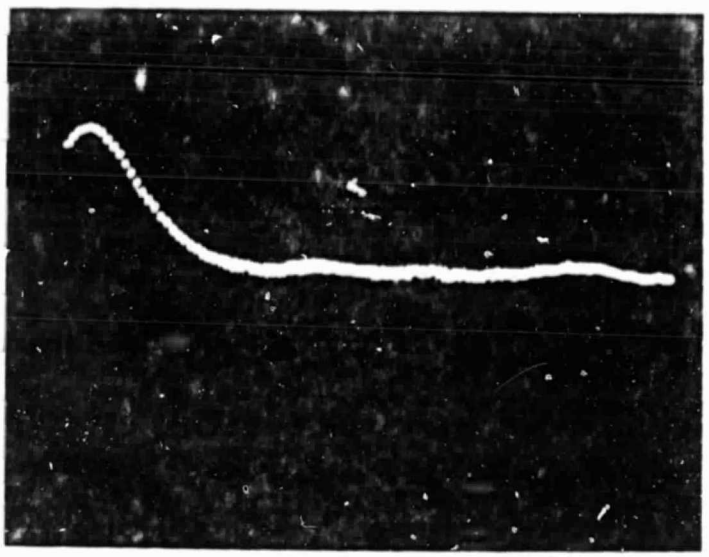

7x1 Delayed, f_D=600KHz, θ=45°

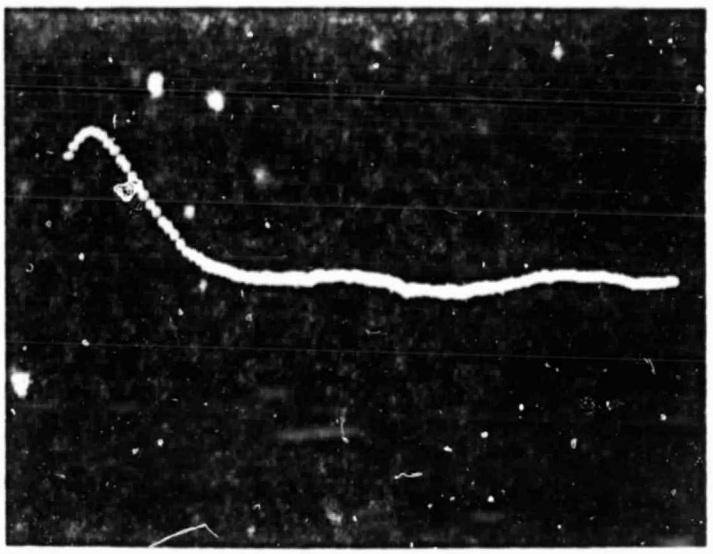

7x4 Delayed, f_D=600KHz, θ=45°

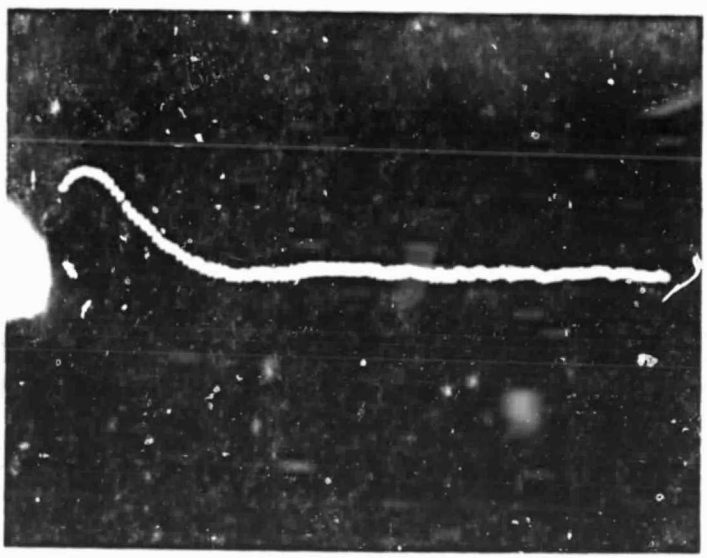

10x4 Delayed, f_D=600KHz, θ=45°

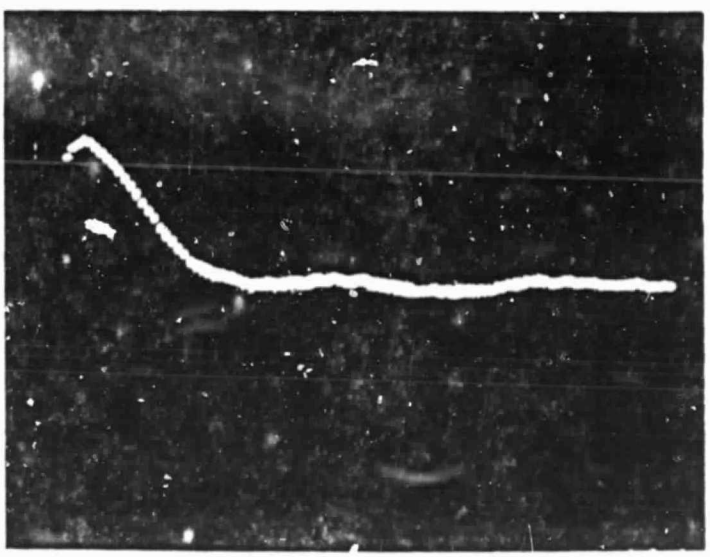

8x7 Delayed, f_D=600KHz, θ=45°

Figure 6. (Continued)

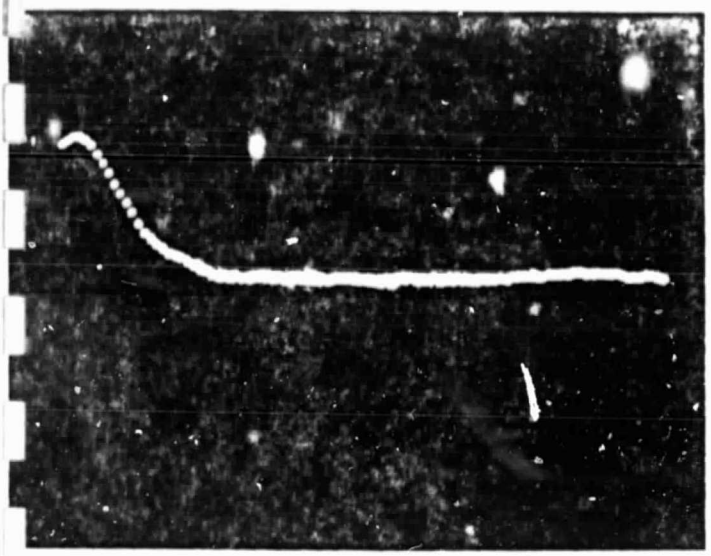

5x3 Delayed, f_D=600KHz, θ=45°

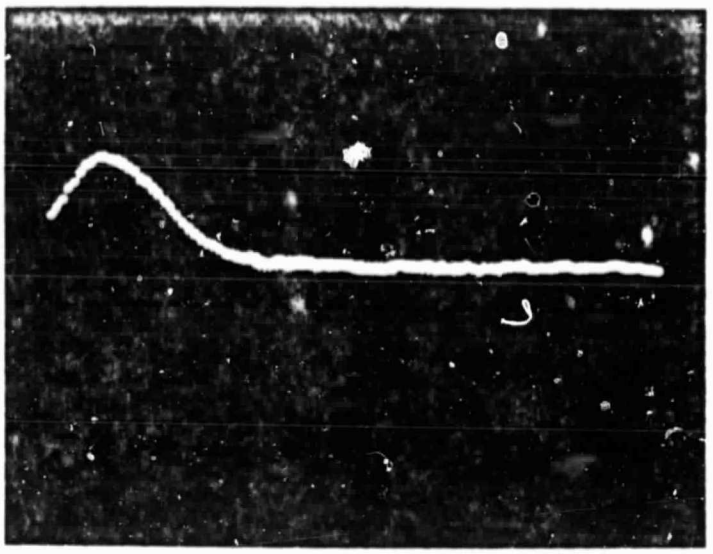

8x5 Delayed, f_D=600KHz, θ=45°

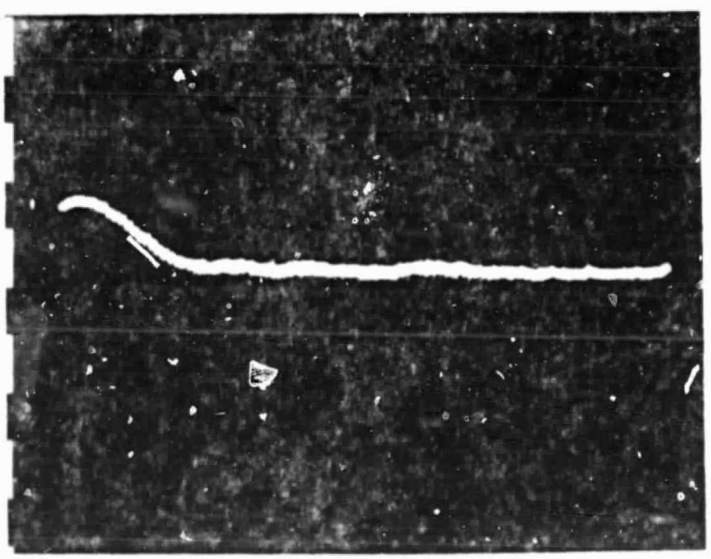

12x5 Delayed, f_D=600KHz, θ=45°

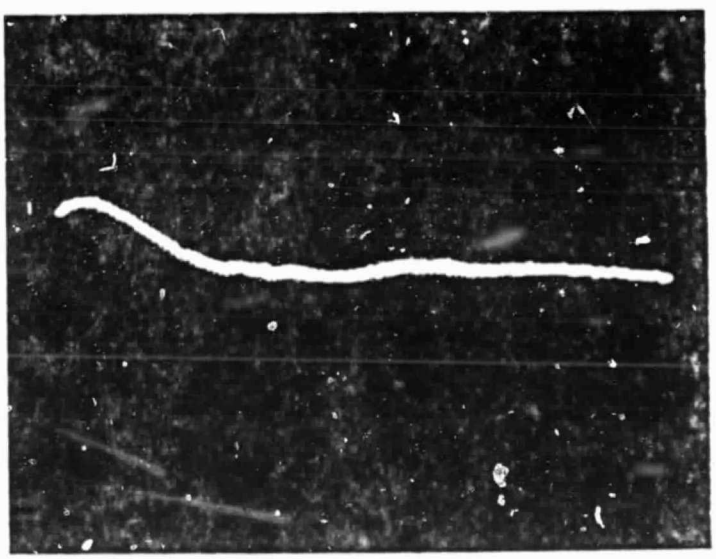

12x3 Delayed, f_D=600KHz, θ=45°

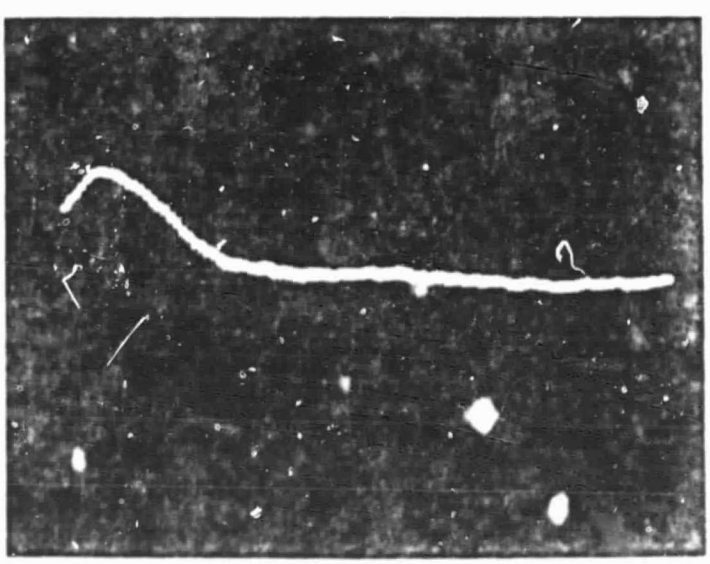

8x12 Delayed,
f_D=600KHz, θ=45°

Figure 6.
(Continued)